Eur. Phys. J. A (2017) **53**: 129
DOI 10.1140/epja/i2017-12319-1

THE EUROPEAN PHYSICAL JOURNAL A

Regular Article – Theoretical Physics

Investigation of the spectroscopy properties of deformed nuclei by combining the X(3) and E(5) models

M. Alimohammadi[a] and H. Hassanabadi

Physics Department, Shahrood University of Technology, Shahrood, Iran

Received: 30 March 2017 / Revised: 12 May 2017
Published online: 20 June 2017 – © Società Italiana di Fisica / Springer-Verlag 2017
Communicated by S. Hands

Abstract. In this paper, we present a model which is composed of two parts related to the special critical points, $E(5)$ (the phase transition between spherical oscillator and γ-soft) and $X(3)$ (a γ-rigid version of $X(5)$). This model is studied to investigate the interplay situations by the free parameter χ. These situations are cited between the γ-unstable and γ-rigid version of the Bohr Hamiltonian. The corresponding wave equation has been considered and the eigenvalues as well as eigenfunctions have been determined by solving this equation. Moreover, we have calculated the energy spectra and transition rates in order to compare our results with experimental data.

1 Introduction

Many physical systems (nuclei, molecules, atomic clusters, etc.) are specified in their equilibrium configuration by a shape [1]. Although, in many cases, these shapes are rigid, there are several situations in which the system undergoes a phase transition between two different shapes [1]. One method to describe these situations is within the framework of algebraic models [2,3]. These models suggest helpful reference concepts such as dynamical symmetries [4,5] which have played an essential role in the spectroscopy of nuclei, in particular in the description of their collective properties [6]. Indeed, a dynamical symmetry corresponds to the Hamiltonian constructed from the Casimir operators of the Lie algebras in a subalgebra chain ($\mathrm{G} \supset \mathrm{G}' \supset \mathrm{G}'' \supset \ldots$) [2,3].

Typical examples of dynamical symmetries in nuclear structure are those defined in the Interacting Boson Model [2] as $U(6)$ symmetry subgroups: $U(5)$, $O(6)$, and $SU(3)$. These algebras identify the limiting cases of the geometric structure: spherical oscillator [$U(5)$], γ-soft rotor [$SO(6)$], and axially symmetric rotor [$SU(3)$] structure [2]. However, the intermediate situations between the structural limits are of the greatest interest, both for applications to actual transitional nuclei [7,8] and in the study of phase transitions between the structural limits [9]. These critical point symmetries [1,10] lead to parameter-independent predictions which are found to be in good agreement with experiment [11–15].

Two critical point symmetries, $E(5)$ [10] and $X(5)$ [1], describe the shape phase transitions $U(5)$-$O(6)$, and respectively $U(5)$-$SU(3)$. These critical points are actually fitting descriptions provided by similarly simple shapes of the potential surface in Bohr model [16] in which the quadrupole shapes are described by using total five variables [17], two associated to the nuclear shape oscillations (β and γ) and three Euler angles θ_i describing the rotational motion.

The $E(5)$ critical-point symmetry has provided the basis for both experimental studies and further theoretical developments [11,18,19]. This model is actually an exact realization of the Euclidean group in five dimensions [6] while the group theoretical structure of the $X(5)$ critical point symmetry, which is materialized in the $N = 90$ isotones ^{150}Nd [20], ^{152}Sm [13], ^{154}Gd [21], and ^{156}Dy [21], is not known. The latter employs two approximations, one related to the separation of variables and the other based on the small angles for the γ shape variable. However, the γ-rigid version of the $X(5)$ model is called $X(3)$ [15]. The γ-rigid condition means a static γdeformation which for the associated quantum Hamiltonian will have a different structure as per Pauli quantization prescription [22]. Also, the $X(3)$ model is described only by the collective coordinate β and two Euler angles because of the assumption related to the γ-rigid condition ($\gamma = 0$).

Recently in refs. [23,24], it was shown that $X(5)$ and $X(3)$ models are partial Euclidean dynamical symmetries [25,26] in the sense that a set of states satisfy exactly the associated symmetrical differential equation. In addition, in ref. [27], a four-dimensional model which shares similar symmetry features emerges by a coherent interplay

[a] e-mail: motahareh.alimohammadi@gmail.com (corresponding author)

of γ-stable and γ-rigid collective conditions [28,29] relating to the $X(5)$ and $X(3)$ models. However, in this paper we consider a Hamiltonian composed of two parts relating to the $X(3)$ and $E(5)$ critical points. This Hamiltonian together with its solution, eigenfunctions as well as eigenvalues is presented in sect. 2 while the corresponding numerical results included in sect. 3. This section involves two parts namely energy spectra (part a) and transition rates (part b), whereas sect. 4 contains a conclusion of the present work.

2 The wave equation

A combined axial symmetric γ-rigid and γ-soft nuclear system is studied by considering the following Hamiltonian [28]:

$$\hat{H} = \chi\hat{T}_1 + (1-\chi)\hat{T}_2 + V(\beta,\gamma), \tag{1}$$

where

$$\hat{T}_1 = -\frac{\hbar^2}{2B}\left(\frac{1}{\beta^2}\frac{\partial}{\partial\beta}\beta^2\frac{\partial}{\partial\beta} + \frac{1}{3\beta^2}\left(\hat{Q}_1^2+\hat{Q}_2^2\right)\right) \tag{2}$$

is the prolate γ-rigid kinetic energy operator [15], and

$$\hat{T}_2 = -\frac{\hbar^2}{2B}\left(\frac{1}{\beta^4}\frac{\partial}{\partial\beta}\beta^4\frac{\partial}{\partial\beta} + \frac{1}{\beta^2}\frac{1}{\sin 3\gamma}\frac{\partial}{\partial\gamma}\sin 3\gamma\frac{\partial}{\partial\gamma} - \frac{1}{4\beta^2}\sum_{k=1}^{3}\frac{\hat{Q}_k^2}{\sin^2\left(\gamma-\frac{2k\pi}{3}\right)}\right) \tag{3}$$

is the same operator corresponding to the usual five-dimensional Bohr Hamiltonian. $\vec{\hat{Q}}$ is the angular-momentum operator from the intrinsic frame of reference with $\hat{Q}_k$ $(k=1,2,3)$ denoting the operators of its projections. The operator $(\hat{Q}_1^2+\hat{Q}_2^2)$ appearing in eq. (2) is written as follows [15]:

$$\left(\hat{Q}_1^2+\hat{Q}_2^2\right) = -\frac{1}{\sin\theta}\frac{\partial}{\partial\theta}\sin\theta\frac{\partial}{\partial\theta} - \frac{1}{\sin^2\theta}\frac{\partial^2}{\partial\phi^2}\,; \tag{4}$$

β and γ are the usual collective coordinates [16], B is the mass parameter and the control parameter χ $(0\le\chi<1)$, which measures the system's γ-rigidity, manages different behaviors of the γ shape variable [27]. The Hamiltonian appearing in eq. (1) clearly operates in a mixed-shape phase space because $\hat{T}_1$ is described in terms of three curvilinear coordinates while $\hat{T}_2$ in five [4]. Thus, the integration measure of this space must be χ-dependent to describe a coherent theory [27]. This deformation of the shape space metric was explained in refs. [29,30].

The main aim of this study is solving the Schrödinger equation associated to eq. (1), as in case of the well-known $E(5)$ model [6], in order to obtain the energy spectra and transition rates. For this purpose, we consider the total wave function as

$$\Psi(\beta,\gamma,\Omega) = \xi(\beta)\varphi(\gamma,\Omega). \tag{5}$$

Therefore, the wave equation for Hamiltonian in eq. (1) can be written as

$$\hat{H}\Psi(\beta,\gamma,\Omega) = E\Psi(\beta,\gamma,\Omega). \tag{6}$$

By substituting eqs. (1) and (5) into eq. (6) and considering a gamma-independent potential

$$V(\beta,\gamma) = V(\beta) \tag{7}$$

one obtains the following separated equations:

$$\left(\hat{Q}_1^2+\hat{Q}_2^2\right)D^L_{M,K}(\Omega) = L(L+1)D^L_{M,K}(\Omega), \tag{8a}$$

$$\left[-\frac{1}{\sin 3\gamma}\frac{\partial}{\partial\gamma}\sin 3\gamma\frac{\partial}{\partial\gamma} + \frac{1}{4}\sum_{k=1}^{3}\frac{\hat{Q}_k^2}{\sin^2(\gamma-\frac{2k\pi}{3})}\right] \times\varphi(\gamma,\Omega) = \Lambda\varphi(\gamma,\Omega), \tag{8b}$$

$$\left[-\frac{\partial^2}{\partial\beta^2} - \frac{2(2-\chi)}{\beta}\frac{\partial}{\partial\beta} + \frac{1}{\beta^2}\left(\chi\frac{L(L+1)}{3} + \Lambda(1-\chi) + (u(\beta)-\varepsilon)\beta^2\right)\right]\xi(\beta) = 0, \tag{8c}$$

where $u(\beta) = \frac{2B}{\hbar^2}V(\beta)$ and $\varepsilon = \frac{2B}{\hbar^2}E$ are reduced potential and energy, respectively.

Equation (8b) was first solved by Bes [31]. The eigenvalue is given as $\Lambda = \tau(\tau+3)$, in terms of the seniority quantum number τ introduced by Rakavy [32] in connection to the eigenvalue of the Casimir operator of the $SO(5)$ symmetry and the eigenfunction is presented as [33]

$$\varphi_{\tau,\bar{\upsilon}_\Delta,L,M}(\gamma,\Omega) = \sum_{\substack{K=0\\ even}}^{L}\eta_{\tau,\bar{\upsilon}_\Delta,L,K}(\gamma)\Phi^L_{M,K}(\Omega), \tag{9}$$

where

$$\Phi^L_{M,K}(\Omega) = \sqrt{\frac{2L+1}{16\pi^2(1+\delta_{K,0})}}\left[D^L_{M,K}(\Omega) + (-1)^L D^L_{M,-K}(\Omega)\right]. \tag{10}$$

In eqs. (9) and (10), $D^L_{M,K}(\Omega)$ is a Wigner function and the notations Ω, $\bar{\upsilon}_\Delta$, L, M and K denote the Euler angles, an additional multiplicity index which is defined more in ref. [2], angular-momentum quantum number, angular-momentum projection on the laboratory z-axis [34] and angular-momentum projection on the body-fixed z-axis [34], respectively.

A potential V (β) which is flat with respect to β allows the nucleus to assume either a spherical $(\beta=0)$ or deformed $(\beta>0)$ shape with minimal energy penalty [6]. Therefore, an idealized approximation near the critical point is the five-dimensional infinite square-well potential [17]:

$$u(\beta) = \begin{cases} 0, & \beta\le\beta_w,\\ \infty, & \beta\ge\beta_w. \end{cases} \tag{11}$$

Substituting this potential and $\xi(\beta) = \beta^{\chi-\frac{3}{2}}f(\beta)$ in eq. (10) one obtains the Bessel equation

$$\left[\frac{\mathrm{d}^2}{\mathrm{d}\beta^2} + \frac{1}{\beta}\frac{d}{d\beta} + \kappa^2 - \frac{\nu^2}{\beta^2}\right]f(\beta) = 0, \tag{12}$$

where

$$\nu = \sqrt{\left(\chi - \frac{3}{2}\right)^2 + \chi\frac{L(L+1)}{3} + \tau(\tau+3)(1-\chi)}, \tag{13a}$$

$$\kappa_{s,\nu}^2 = \varepsilon_{s,\nu}. \tag{13b}$$

Thus the eigenvalues of eq. (8) can be written as follows:

$$E_{s,\tau,L} = \frac{\hbar^2}{2B}\left(\frac{x_{s,\nu}}{\beta_w}\right)^2, \tag{14}$$

where $x_{s,\nu}$ is the sth zero of the Bessel function of the first kind $J_\nu(\frac{x_{s,\nu}}{\beta_w}\beta)$, $s = n_\beta + 1$ and $n_\beta = 0, 1, \ldots$. The solution of eq. (10) is then

$$\xi_{s,\tau,L}(\beta) = C_{s,\nu}\beta^{\chi-\frac{3}{2}} J_\nu\left(\frac{x_{s,\nu}}{\beta_w}\beta\right), \tag{15}$$

where $C_{s,\nu}$ is determined by calculating the following integral:

$$\int_0^{\beta_w} \left[\xi_{s,\tau,L}(\beta)\right]^2 \beta^{4-2\chi} \mathrm{d}\beta = 1. \tag{16a}$$

By using this relation together with the properties of the Bessel function, we reach to the final form of the normalization constant

$$C_{s,\nu} = \frac{1}{\frac{\beta_w}{\sqrt{2}}\left[J_{\nu+1}(x_{s,\nu})\right]}. \tag{16b}$$

It should be noticed that in ref. [27] the same eq. (12) occurs, but with $\nu = \sqrt{(\chi - \frac{3}{2})^2 + \frac{L(L+1)}{3}}$, so it can be seen that in ref. [27], the limiting cases of $X(3)$ and $X(5)$ happens for $\chi = 1$ and $\chi = 0$ while in our case $X(3)$ and $E(5)$ appears which is simply obtained from (13a). The reason for this discrepancy is that the potential $V(\beta, \gamma)$ is different in the two studies. Indeed, the critical point symmetries, like $E(5)$ or $X(5)$, are actually fitting descriptions provided by similarly simple shapes of the potential surface in the Bohr model.

Finally, the total wave function is given by the product of angular, β and γ wave functions

$$\begin{aligned}\Psi(\beta,\gamma,\Omega) = {} & C_{s,\nu}\beta^{\chi-\frac{3}{2}} J_\nu\left(\frac{x_{s,\nu}}{\beta_w}\beta\right) \sum_{\substack{K=0\\ even}}^{L} \eta_{\tau,\tilde{\nu}_\Delta,L,K}(\gamma) \\ & \times\sqrt{\frac{2L+1}{16\pi^2(1+\delta_{K,0})}}\left[D^L_{M,K}(\Omega)\right. \\ & \left. + (-1)^L D^L_{M,-K}(\Omega)\right]. \end{aligned} \tag{17}$$

3 Numerical results

3.1 Energy spectrum

To determine the energy spectra, we normalize eq. (14) as follows:

$$\begin{aligned} A\left(E_{1,0,0}\right)_H + B &= 0, \\ A\left(E_{1,1,2}\right)_H + B &= 1. \end{aligned} \tag{18}$$

Indeed, we normalize the energy of the first and second levels of the ground-state band to zero and one, respectively, so the normalized energy for each state labeled by the quantum numbers $s(s = n_\beta + 1)$, τ and L takes the form

$$\tilde{E}_{s,\tau,L} = \frac{x^2_{s,\tau,L} - x^2_{1,0,0}}{x^2_{1,1,2} - x^2_{1,0,0}}. \tag{19}$$

As is obvious from eqs. (14) and (13a), the only free parameter to determine the energy spectra is the control parameter χ. In order to see the evolution of the several normalized energy levels $[(\tau, L, n) = (1,2,0), (2,2,0), (2,4,0), (0,0,1), (2,4,1), (3,6,0), (4,8,0), (3,4,0), (3,3,0), (3,0,0), (1,2,1), (2,2,1), (4,6,0), (4,5,0), (4,4,0), (4,2,0)]$ as a function of the control parameter, we have depicted fig. 1. In this figure, one can see the relevant evolution in five parts (a, b, c, d and e) corresponding to the five values adopted for the control parameter ($\chi = 0, 0.25, 0.50, 0.75$ and 0.95). It is obviously seen that inserting the parameter χ removes the degeneracy on the energy levels related to the $E(5)$ model ($\chi = 0$), the splits increase with increasing the value of χ and the relevant energy levels shift to the first level of the ground-state band. It should be also mentioned that the different columns of fig. 1 correspond to the different bands of a nucleus. In other words, the "first"; "second and third"; "fourth and fifth"; "sixth"; "seventh" columns correspond to the "ground-state band"; "γ-band ($K = 2$)"; "band based on 0^+"; "first β-band"; "band maybe based on 2^+", respectively. The band based on 0^+ has been experimentally observed. For instance, in ^{110}Pd nucleus, the values related to the normalized energy levels of this band are as follows [35]: 2.53, 3.25 and 4.60 corresponding to 0^+, 2^+ and 4^+, respectively.

On the other hand, we have implemented the fitting procedure for the normalized energy in a way that our results for each nucleus have the best agreement to the relevant experimental data or the standard error has the minimum value. This statistical error is defined as follows:

$$\sigma = \sqrt{\frac{1}{N-1}\sum_{i=1}^{N}\left[\left(\tilde{E}_{s,\tau,L}\right)_{th} - \left(\tilde{E}_{s,\tau,L}\right)_{\exp}\right]^2_i}, \tag{20}$$

where N denotes the number of available experimental data for each nucleus. The obtained results together with the parameters N, χ and σ are reported in table 1. In this table our theoretical results are compared with the experimental data through the value of σ. As one can see, there are a rather good agreement between our results and the experimental data. Indeed, the value of statistical error for each of nucleus is equal to or smaller than one. The best agreement to the experimental data belongs to the ^{126}Xe, ^{110}Pd, ^{128}Xe and ^{114}Pd nuclei. Moreover, it should be mentioned that the notations "–", "( )" and "[ ]" relate to the cases in which "the relevant experimental data is not available", "we are not sure about the reported data" and "the data is related to the backbending phenomena [36]". This kind of data has been ignored in the fitting procedure because further out there is a backbending (the energy

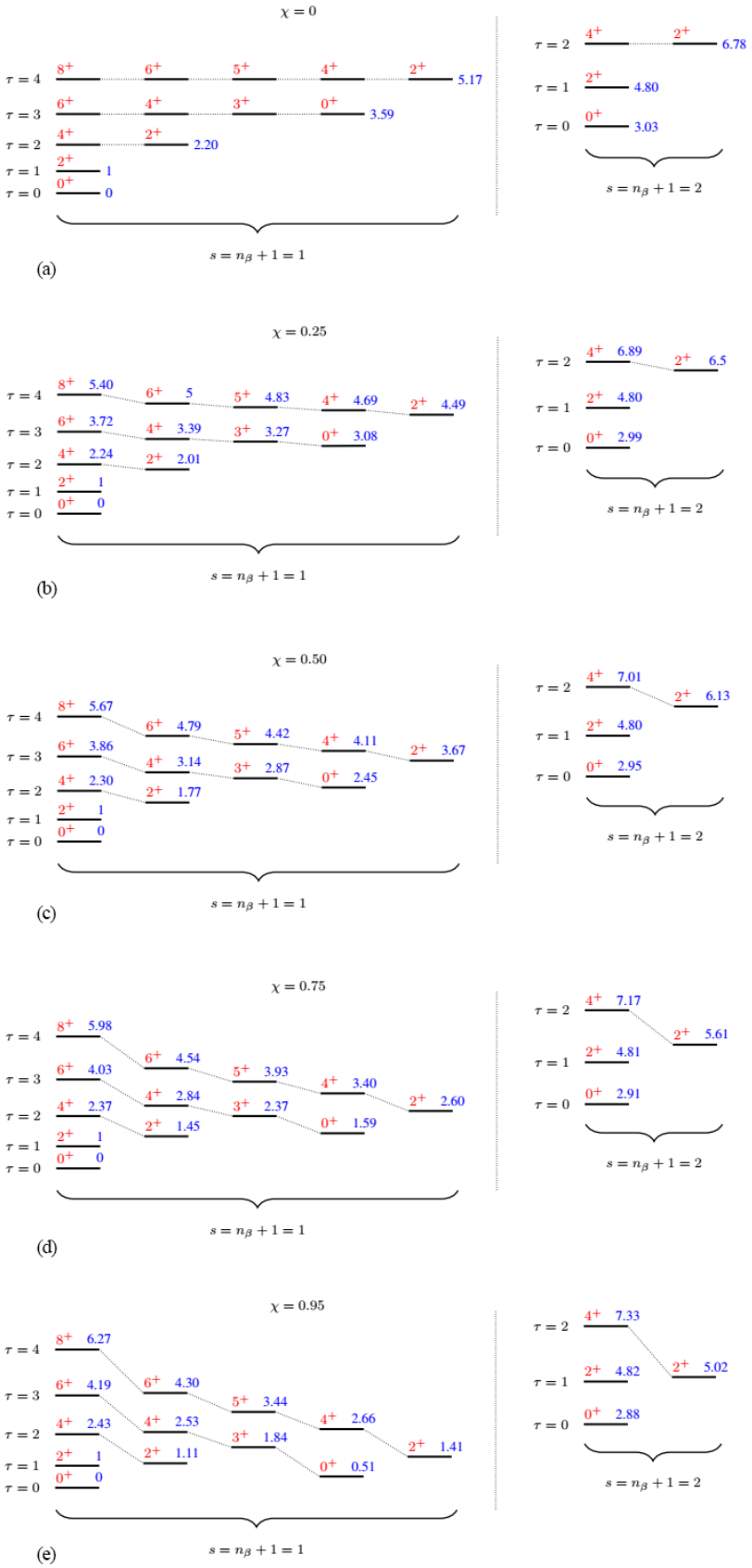

Fig. 1. The evolution of the several normalized energy levels as a function of the control parameter χ. Red and blue colors specify the angular-momentum quantum number L and the normalized energy values, respectively.

Table 1. The theoretical normalized energy (upper line) for some levels of ground state, the first β band and the first γ band compared with the available experimental data (lower line) [35].

$\tilde{E}_{s,\tau,L}$	^{100}Ru	^{104}Ru	^{110}Pd	^{112}Pd	^{114}Pd	^{116}Pd	^{118}Xe	^{120}Xe	^{122}Xe	^{124}Xe	^{126}Xe [35,37]	^{128}Xe
$\tilde{E}_{1,2,4}$	2.23	2.24	2.25	2.25	2.23	2.21	2.20	2.20	2.22	2.23	2.25	2.25
	2.27	2.48	2.46	2.53	2.56	2.58	2.40	2.47	2.50	2.48	2.42	2.33
$\tilde{E}_{1,3,6}$	3.67	3.69	3.73	3.74	3.68	3.61	3.59	3.59	3.66	3.67	3.72	3.74
	3.85	4.35	4.21	4.45	4.51	4.58	4.14	4.33	4.43	4.37	4.21	3.92
$\tilde{E}_{1,4,8}$	5.33	5.36	5.43	5.45	5.34	5.20	5.17	5.17	5.30	5.33	5.41	5.45
	5.67	6.48	6.14	6.65	6.66	6.89	6.15	6.51	6.69	6.58	6.27	5.67
$\tilde{E}_{1,5,10}$	7.18	7.24	7.35	7.33	7.20	6.99	6.93	6.93	7.14	7.18	7.32	7.37
	7.85	8.69	8.21	8.75	[8.60]	–	8.35	8.90	9.18	8.96	8.64	[7.22]
$\tilde{E}_{2,0,0}$	3.01	3.00	2.99	2.99	3.00	3.03	3.03	3.03	3.01	3.01	2.99	2.99
	2.10	(2.76)	2.53	3.27	2.62	3.26	2.46	2.82	3.47	3.58	3.38	3.57
$\tilde{E}_{2,1,2}$	4.80	4.80	4.80	4.80	4.80	4.80	4.80	4.80	4.80	4.80	4.80	4.80
	3.46	4.23	3.25	4.02	4.18	–	3.64	3.95	4.51	4.60	4.32	4.51
$\tilde{E}_{2,2,4}$	6.85	6.87	6.90	6.91	6.85	6.80	6.78	6.78	6.84	6.85	6.89	6.91
	4.36	5.81	4.60	4.92	–	–	5.13	5.31	–	5.69	5.25	(5.39)
$\tilde{E}_{1,2,2}$	2.07	2.04	1.98	1.97	2.06	2.17	2.20	2.20	2.10	2.07	2.00	1.97
	2.52	2.49	2.18	2.11	2.09	2.17	2.75	2.72	2.55	2.39	2.26	2.19
$\tilde{E}_{1,3,3}$	3.38	3.32	3.22	3.21	3.36	3.54	3.59	3.59	3.42	3.38	3.25	3.21
	3.49	3.47	3.24	3.14	3.04	3.13	4.05	3.94	3.67	3.59	3.39	3.23
$\tilde{E}_{1,3,4}$	3.46	3.42	3.36	3.35	3.45	3.56	3.59	3.59	3.48	3.46	3.38	3.35
	3.82	4.20	3.74	3.91	3.97	4.04	4.27	4.34	4.23	4.06	3.83	3.62
$\tilde{E}_{1,4,5}$	4.94	4.89	4.79	4.77	4.93	5.12	5.17	5.17	4.99	4.94	4.82	4.77
	4.78	5.23	4.71	5.04	4.90	5.05	5.70	5.63	5.36	5.19	4.90	4.51
$\tilde{E}_{1,4,6}$	5.05	5.03	4.97	4.97	5.05	5.14	5.17	5.17	5.08	5.05	4.99	4.97
	5.01	–	5.32	5.74	5.94	6.17	5.92	6.15	6.21	6.06	5.70	5.15
$\tilde{E}_{1,5,7}$	6.72	6.67	6.58	6.56	6.71	6.89	6.93	6.93	6.76	6.72	6.60	6.56
	6.39	7.33	–	7.12	6.88	7.32	7.59	7.63	7.42	7.27	6.85	–
$\tilde{E}_{1,5,8}$	6.86	6.84	6.81	6.80	6.86	6.92	6.93	6.93	6.87	6.86	6.82	6.80
	6.58	7.95	7.09	7.57	7.98	8.35	7.78	8.23	8.44	8.23	7.88	6.72
N	14	12	13	14	12	11	14	14	13	14	14	11
χ	0.17	0.21	0.28	0.29	0.18	0.04	0	0	0.14	0.17	0.26	0.29
σ	0.88	0.85	0.90	0.90	0.71	0.88	0.91	1.0	1.0	0.91	0.77	0.28

difference between consecutive energy levels is no longer monotonically increasing) which suggests that higher spin states are no longer purely collective. Moreover, the reason for the selection of this kind of levels in table 1, the levels up to $L = 10$ and $L = 8$ in the ground state and the γ-band respectively, is the backbending phenomena.

Furthermore, in table 1, it is obviously seen that for the xenon isotopes the parameter χ increases with increasing the mass number. It may be means that nuclei (only for the xenon isotopes) with lower mass number can be investigated through the $E(5)$ model while the nuclei with more mass number by the $X(3)$ model.

3.2 Transition rates

In general, the quadrupole transition operator is [15,38]

$$T^{(E2)}_{\mu} = t\alpha_{\mu} = t\beta\Big[D^{2}_{\mu,0}(\Omega)\cos\gamma + \frac{1}{\sqrt{2}}\big[D^{2}_{\mu,2}(\Omega) + D^{2}_{\mu,-2}(\Omega)\big]\sin\gamma\Big], \tag{21}$$

where Ω denotes the Euler angles and t is a scale factor. By employing this operator together with the eq. (17), one can reach to the $E2$ transition probability which has the

Table 2. Several $B(E2)$ ratios (upper line) of nuclei in table 1 compared to the experimental data [35] (lower line). All transition values are normalized to$1,1,2 \rightarrow 1,0,0$. The errors relate to the experimental errors [35].

$s,\tau,L \rightarrow s',\tau',L'$	^{100}Ru	^{104}Ru	^{110}Pd	^{112}Pd	^{114}Pd	^{116}Pd	^{118}Xe	^{120}Xe	^{122}Xe	^{124}Xe	^{126}Xe	^{128}Xe
$1,2,4 \rightarrow 1,1,2$	1.70	1.70	1.72	1.72	1.70	1.68	1.67	1.67	1.69	1.70	1.71	1.72
	1.4±0.1	1.4±0.1	1.6±0.1	–	–	–	1.1	1.15	1.5	1.17	–	1.35±0.25
$1,3,6 \rightarrow 1,2,4$	2.22	2.23	2.25	2.26	2.22	2.18	2.17	2.17	2.21	2.22	2.25	2.26
	< 4.6±0.1	–	1.95	–	–	–	0.9±0.2	1.15	1.5	1.52±0.10	–	1.33±0.24
$1,4,8 \rightarrow 1,3,6$	2.62	2.64	2.68	2.68	2.63	2.57	2.55	2.55	2.61	2.62	2.67	2.68
	–	–	–	–	–	–	0.45	0.95	1.0	1.14±0.33	–	2.04±0.23
$1,5,10 \rightarrow 1,4,8$	2.95	2.97	3.01	3.02	2.95	2.88	2.86	2.86	2.93	2.95	3.00	3.02
	–	–	–	–	–	–	> 0.75	0.9±0.1	1.5	0.36±0.04	–	$5.28\pm1.21\times10^{-4}$
$2,1,2 \rightarrow 2,0,0$	0.76	0.76	0.76	0.76	0.76	0.75	0.75	0.75	0.76	0.76	0.76	0.76
	0.9	–	–	–	–	–	–	–	–	–	–	–
$2,2,4 \rightarrow 2,1,2$	1.26	1.26	1.27	1.27	1.26	1.25	1.24	1.24	1.26	1.26	1.27	1.27
	–	–	–	–	–	–	–	–	–	–	–	–
$1,2,2 \rightarrow 1,1,2$	1.69	1.70	1.71	1.71	1.70	1.68	1.67	1.67	1.69	1.69	1.71	1.71
	0.9	0.95	0.8	–	–	–	–	–	–	0.55±0.09	–	1.23±0.20
$1,3,4 \rightarrow 1,2,2$	1.15	1.15	1.15	1.16	1.15	1.14	1.14	1.14	1.15	1.15	1.15	1.16
	–	–	0.6±0.1	–	–	–	–	–	–	1.2±0.4	–	0.6±0.1
$1,3,3 \rightarrow 1,2,2$	1.57	1.57	1.58	1.58	1.57	1.55	1.55	1.55	1.56	1.57	1.57	1.58
	0.3±0.1	–	–	–	–	–	–	–	–	0.16±0.06	–	4.50
$1,3,4 \rightarrow 1,2,4$	1.05	1.06	1.07	1.07	1.06	1.04	1.03	1.03	1.05	1.05	1.07	1.07
	0.8±0.5	–	0.6±0.1	–	–	–	–	–	–	0.58±0.21	–	0.61±0.07

following form [39]:

$$B\left(E2; s\tau L \rightarrow s'\tau' L'\right) = t^2\left(\tau', L'; 1, 2 \| \tau, L\right)^2 \times \left[\langle \tau \| \| \alpha \| \| \tau' \rangle I_{s\tau L; s'\tau' L'}\right]^2, \quad (22)$$

where $(\tau_1, L_1; \tau_2, L_2 \| \tau_3, L_3)$ is the $SO(5)$ Clebsch-Gordan coefficient whose usually encountered values are tabulated in ref. [33] and the corresponding non-vanishing reduced matrix element has the following simple form [40,41]:

$$\langle \tau \| \| \alpha \| \| \tau' \rangle = \sqrt{\frac{\tau}{2\tau+3}}\delta_{\tau,\tau'+1} + \sqrt{\frac{\tau+3}{2\tau+3}}\delta_{\tau,\tau'-1} \quad (23)$$

while I is the integral over the β shape variable

$$I_{s\tau L; s'\tau' L'} = \int_0^\infty \beta \xi_{s\tau L}(\beta)\xi_{s'\tau' L'}(\beta)\beta^{4-2\chi} \mathrm{d}\beta. \quad (24)$$

Some transition rates for nuclei presented in table 1 have been calculated by using eq. (22). The obtained results are shown in table 2. In this table, in order to evaluate our results, we compared them with the relevant available experimental data. There is a rather good agreement between our data and the experimental one. As is expected, the transition rates related to the levels of the ground state band for all nuclei in table 2 take place between the $E(5)$ and $X(3)$ models. This subject can be seen by comparing the values of table 2 with the results of refs. [6] and [15].

4 Conclusion

In summary, we considered a mixed Hamiltonian composed of two parts related to the $E(5)$ and $X(3)$ models. The exact expressions for the eigenvalues and eigenfunctions of the corresponding wave equation were also presented. Moreover, we calculated the normalized energies and transition rates. The corresponding results have been reported in tables 1 and 2, respectively. As we know, one of the disadvantages of the $X(3)$ model is that it cannot predict the energy spectra related to the levels of γ-bands. However, the $X(3)$ model should be considered as a separate case which cannot be achieved in the present formalism as a limiting model without considering the modification of the Bohr symmetry restrictions on the parity of the angular momentum states. On the other hand, since in the $E(5)$ model the normalized energy is depend on the seniority quantum number τ and the quantum number n_β(s), it suggests the same energy values for different levels like levels with $L = 3$ and $L = 4$ of the γ-band while the experimental data do not show this degeneracy. But, when we combine the $X(3)$ and $E(5)$ models, as we have done in this work, these two problems will disappear. This point is clearly seen in fig. 1 and table 1.

It is a great pleasure for the authors to thank the referees for their helpful comments.

References

1. F. Iachello, Phys. Rev. Lett. **87**, 052502 (2001).
2. F. Iachello, A. Arima, *The Interacting Boson Model* (Cambridge University Press, Cambridge, 1987).
3. F. Iachello, R.D. Levine, *Algebraic Theory of Molecules* (Oxford University Press, Oxford, 1995).
4. F. Iachello, in *Group Theoretical Methods in Physics*, edited by W. Beiglböck, A. Bohm, E. Takasugi, Lect. Notes Phys. Vol. **94** (Springer-Verlag, Berlin, 1979) p. 420.
5. F. Iachello, *Lie Algebras and Applications*, Lect. Notes Phys. Vol. **708** (Springer, Berlin, 2006).
6. M.A. Caprio, F. Iachello, Nucl. Phys. A **781**, 26 (2007).
7. O. Scholten, F. Iachello, A. Arima, Ann. Phys. (N.Y.) **115**, 325 (1978).
8. R.F. Casten, M. Wilhelm, E. Radermacher, N.V. Zamfir, P. von Brentano, Phys. Rev. C **57**, R1553 (1998).
9. D.H. Feng, R. Gilmore, S.R. Deans, Phys. Rev. C **23**, 1254 (1981).
10. F. Iachello, Phys. Rev. Lett. **85**, 3580 (2000).
11. R.F. Casten, N.V. Zamfir, Phys. Rev. Lett. **85**, 3584 (2000).
12. R.M. Clark *et al.*, Phys. Rev. C **69**, 064322 (2004).
13. R.F. Casten, N.V. Zamfir, Phys. Rev. Lett. **87**, 052503 (2001).
14. R.M. Clark *et al.*, Phys. Rev. C **68**, 037301 (2003).
15. D. Bonatsos *et al.*, Phys. Lett. B **632**, 238 (2006).
16. A. Bohr, Mat. Fys. Medd. K. Dan. Vidensk. Selsk. **26**, 14 (1952).
17. L. Wilets, M. Jean, Phys. Rev. **102**, 788 (1956).
18. R. Fossion, D. Bonatsos, G.A. Lalazissis, Phys. Rev. C **73**, 044310 (2006).
19. D. Bonatsos, D. Lenis, N. Minkov, P.P. Raychev, P.A. Terziev, Phys. Rev. C **69**, 044316 (2004).
20. R. Krücken *et al.*, Phys. Rev. Lett. **88**, 232501 (2002).
21. A. Dewald *et al.*, Eur. Phys. J. A **20**, 173 (2004).
22. W. Pauli, *Handbuch der Physik*, Vol. **XXIV/1** (Springer-Verlag, Berlin, 1933).
23. D. Bonatsos, E.A. McCutchan, R.F. Casten, Phys. Rev. Lett. **101**, 022501 (2008).
24. D. Bonatsos *et al.*, Phys. Rev. C **80**, 034311 (2009).
25. Y. Alhassid, A. Leviatan, J. Phys. A **25**, L1265 (1992).
26. A. Leviatan, Phys. Rev. Lett. **98**, 242502 (2007).
27. R. Budaca, A.I. Budaca, Phys. Lett. B **759**, 349 (2016).
28. R. Budaca, A.I. Budaca, J. Phys. G: Nucl. Part. Phys. **42**, 085103 (2015).
29. R. Budaca, A.I. Budaca, Eur. Phys. J. A **51**, 126 (2015).
30. R. Budaca, A.I. Budaca, Phys. Rev. C **94**, 054306 (2016).
31. D.R. Bes, Nucl. Phys. **10**, 373 (1959).
32. G. Rakavy, Nucl. Phys. **4**, 289 (1957).
33. D.J. Rowe, P.S. Turner, J. Repka, J. Math. Phys. **45**, 2761 (2004).
34. L. Fortunato, Eur. Phys. J. A **26**, 1 (2005).
35. `http://www.nndc.bnl.gov/ensdf`.
36. P. Ring, P. Shuck, *The Nuclear Many-Body Problem* (Springer-Verlag, New York, 1980).
37. C. Rønn Hansen *et al.*, Phys. Rev. C **76**, 034311 (2007).
38. R.F. Casten, N.V. Zamfir, Phys. Rev. Lett. **87**, 052503 (2001).
39. R. Budaca, Eur. Phys. J. A **52**, 314 (2016).
40. D.J. Rowe, J. Phys. A: Math. Gen. **38**, 10181 (2005).
41. D.J. Rowe, P.S. Turner, Nucl. Phys. A **753**, 94 (2005).